We are IntechOpen, the world's leading publisher of Open Access books Built by scientists, for scientists

4,800
Open access books available

122,000
International authors and editors

135M
Downloads

Our authors are among the

154
Countries delivered to

TOP 1%
most cited scientists

12.2%
Contributors from top 500 universities

WEB OF SCIENCE™

Selection of our books indexed in the Book Citation Index in Web of Science™ Core Collection (BKCI)

Interested in publishing with us?
Contact book.department@intechopen.com

Numbers displayed above are based on latest data collected.
For more information visit www.intechopen.com

Chapter

Photocatalytic Adsorbents Nanoparticles

Gustavo Lopes Colpani, Adrieli Teresinha Odorcik Dal'Toé, Micheli Zanetti, Rubieli Carla Frezza Zeferino, Luciano Luiz Silva, Josiane Maria Muneron de Mello and Márcio Antônio Fiori

Abstract

Photocatalysis and high adsorption coupling in a same nanoparticle have been emerged as a prominent class of cost-effective materials to degrade recalcitrant contaminants in wastewater. α-Hematite, metal-organic frameworks and TiO_2 nanocomposites have been investigated due to their features that overcome the other conventional photocatalysts and adsorbents to remove contaminants in aqueous medium. Several methods are applied to synthesize these nanostructures with different properties and physicochemical features and a brief review is shown to these well-established techniques to provide an understanding for the construction and application of these advanced materials.

Keywords: photocatalytic adsorbents, α-hematite, metal-organic frameworks, TiO_2, nanoparticles

1. Introduction

Most conventional technologies applied to the removal of contaminants dispersed in the aqueous effluent employ the adsorption techniques. However, a class of contaminants, not yet regulated in relation to disposal parameters and/or presence in the environment by the government agencies, may have potentially harmful effects on aquatic biota and humans. However, the adsorption techniques need to be investigated in the removing processes of an important class of contaminants that not yet was regulated in relation to discard in the environment by the government agencies, but that have potentially harmful effects on aquatic biota and humans. These emerging contaminants may be synthetic or natural and their most prominent compounds are the drugs, the personal care products, hormones, flame retardants, perfluoroalkylated substances and pesticides [1, 2]. These compounds are called emerging contaminants and their nomenclature originates from the low concentrations detected in surface waters ($\mu g \bullet l^{-1}$ or $ng \bullet l^{-1}$) [3, 4]. The incidences in very small quantities could only be identified in the last 20 years, due to the appearance of new analytical equipment [5].

Compounds of difficult degradation by conventional sewage processes can affect the lives of millions of people due to contamination of water resources [6]. The incidence of recalcitrant molecules introduced into water resources is a serious problem of toxicity and deserves the development and research of specific affluent and effluent treatment systems, with greater process efficiency, greater safety and lower costs [7, 8]. Physicochemical and biological methods currently employed are capable of degrading some of these compounds, but they have a high-cost application, which makes it difficult to implement in regions with limited financial resources [9]. Furthermore, these methods can generate complex residues for treatment or storage, such as sludge and toxic or recalcitrant compounds. [10]

Thus, alternative methods have been researched in an attempt to eliminate these contaminants effectively, as the adsorption techniques. The adsorption methods have some important vantages: can be operated with low energy consumer and with low operational cost, and cannot generate secondary compounds [11, 12]. The adsorbents applied in the adsorption techniques must have a high surface area, an adequate pore density and surface charge capable of interacting with specific compounds to be removed from the aqueous solution, which makes assure a high removal capacity [13, 14]. These adsorbents are produced from a variety of sources, such as clays, zeolites, silica and carbonaceous materials, which can be applied directly or after chemically or physically activation [15].

However, these processes need be improved because additional costs are still necessary for the waste disposals or for the regeneration of the adsorbents [16]. But recent combinations with other technologies have been reported to improve the removal of the organic pollutants from the water by nanoparticles adsorbents. One of the most attractive methods with nanoparticles is the combination of the adsorption processes and the advanced oxidation processes (AOPs) to ensure high efficient for the capture and for the degradation of the contaminants [17]. Advanced oxidative processes are characterized mainly by the production of •OH radicals in the reaction media or on the catalyst surface of the nanoparticles, which are oxidative species with high redox potential (E^0 = 2.80 V). Due to this feature, these radicals have capacity to degrade a great variety of organic compounds, transforming them into smaller molecules or reducing them completely in carbon dioxide (CO_2) and water (H_2O), mineralizing them [18, 19].

Among the advanced oxidation process, heterogeneous photocatalysis is widely researched with the nanoparticles adsorbents. In this process, very reactive oxygen species (•OH, $^1O_2$ e $•O_2^-$) are generated from the use of semiconductor catalysts nanostructures induced by ultraviolet or visible radiation [20]. The semiconductors capacity to absorb energy and degrade molecules is due to the energy bands created by atomic orbitals arranged when a new compound is formed on the surfaces of the nanoparticles. These regions are denominated conduction band (CB) and valence band (VB) [21]. In the semiconductors, there will be a region without available energy levels, which are described as band gap [22]. In these cases, only the nanoparticles will be a catalyst if an amount of energy equal or greater than the band gap is provided, which will allow electrons transfer from valence band to conduction band, as depicted in **Figure 1**. The electron (e^-) in the CB can interact with oxygen molecules and form reactive groups, such as the hydroxyl (•OH) and superoxide ($•O_2^-$) radicals and singlet oxygen ($^1O_2$) [23–25]. On the other hand, the vacancies (h^+) created due to the electrons transfer are oxidants with potential to convert water molecules in •OH [26].

Therefore, a nanoparticle that can combine the adsorption affinity with photocatalysis will give rise to novel materials, which would join the advantages of both techniques to degrade organic pollutants, instead of only change the phase of these contaminants [27, 28]. The major photocatalytic adsorbents researched are α-hematite (Fe_2O_3), meta-organic frameworks (MOFs) and TiO_2 nanocomposites, which are described further.

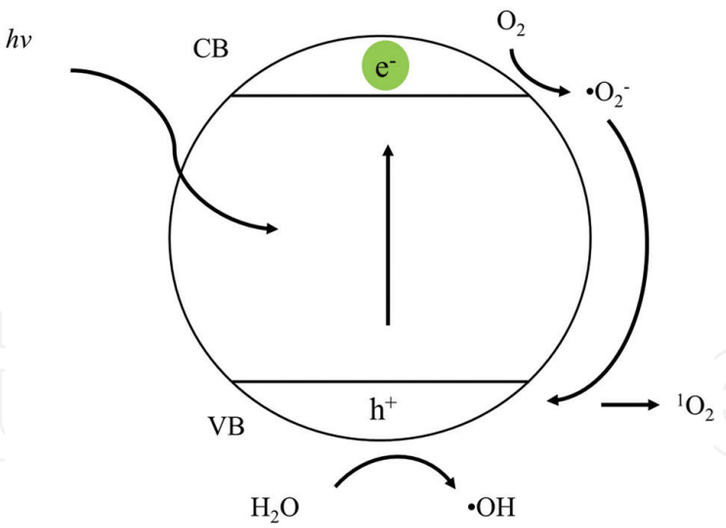

Figure 1.
Semiconductors photocatalytic mechanism.

2. α-Hematite (Fe_2O_3)

Hematite is the most thermodynamically stable phase of iron oxide and is formed by a hexagonal crystalline structure. It is used in catalysis processes and as pigments, in the lithium ion batteries and for the water treatment as an adsorbent [29, 30]. The strong adsorption capacity of organic and inorganic species by the hematite is related to its intrinsic chemical and electronic properties [31, 32]. The pH ZPC of the hematite is approximately 8.0, which implies that in aqueous media with pH below 8.0, the surface is positively charged and the interaction between anionic molecules is stronger [30, 31].

This semiconductor is also employed in photocatalysis due to its reduced band gap energy (E^0 = 2.2 eV), which allows the visible light absorption and with an energy level higher than water oxidation potential. Moreover, the α-Fe_2O_3 phase is a material with low cost and environment friendly and has good chemical and corrosion stability [33]. It is found that because of these characteristics, the hematite nanoparticles are potential candidates to good adsorbents for the removal of contaminants from aqueous systems.

Many methods have been researched and applied to produce hematite nanoparticles, but the most common techniques are the thermal decomposition, sol-gel, solvothermal and hydrothermal [34–36]. These different methodologies are used to control parameters like size, shape and crystal structure of the particles produced, with the aim to ensure interesting adsorption capacity and photocatalysis [37].

Thermal decomposition usually applies inorganic salts, such as nitrates, oxalates and chlorides, with low thermal stability to produce metal oxide nanoparticles in air atmosphere [38]. However, this process can be accomplished by calcination of magnetite (Fe_3O_4) or maghemite (γ-Fe_2O_3) at 500°C [39]. Al-Gaashani et al. [40] synthesized hematite by thermal decomposition of iron (III) nitrate 9-hydrate at different temperatures (300, 400, 500 and 600°C) under ambient conditions within a short time (20 min). The nanostructures showed crystallite sizes in a range to 10–30 nm with high surface area and optical band gap near 3.0 eV. The iron oxide α-Fe_2O_3 nanoparticles with different crystalline structure were prepared by [41], which calcinated the iron precursor ferric ammonium citrate at different temperatures (300, 400 and 550°C) under air atmosphere. The mean particle sizes of the samples were near 20 nm with excellent dye photocalytic degradation under visible light after 10 h. Yang et al. [42] applied direct thermal decomposition of goethite

(α-FeOOH, calcinated at 300°C, to produce hematite with a high adsorption capacity for arsenic (14.5 $mg \bullet g^{-1}$).

In the sol-gel method, a metal salt, usually chloride and nitrate, is dispersed in alcohol solution to form the "sol" phase by hydrolysis, condensation and polymerization. The "sol" phase is heated to evaporate the solvent and this mixture is converted to "gel" phase, which is composed for regular nanoparticles [43, 44]. Xiao et al. [45] evaluated the adsorption of chromium (VI) on hematite nanoparticles produced by sol-gel technique. The precursors used to form hematite were $FeCl_3 \cdot 6H_2O$ and $(NH_4)_2CO_3$ dissolved in water and ethanol. The crystalline size of α-Fe_2O_3 nanoparticles samples showed values between 15 and 30 nm, with a removal efficiency of chromium near 50% to smaller particles. Sol-gel method was applied by [46] to form hematite nanoparticles from $Fe(NO_3)_3 \bullet 9H_2O$ dispersed in ethanol. The particles produced by this method possess sizes below 10 nm and excellent optical properties, with a band gap energy near 2 eV. Raja et al. [47] employed ferric nitrate dissolved in ethylene glycol to produce hexagonal nanoparticles with interesting structural, optical and magnetic properties. The photocatalytic properties of hematite produce by sol-gel technique were evaluated by [44], that used $Fe(NO_3)_3 \bullet 9H_2O$ dispersed in ethylene glycol to form nanoparticles with a crystalline size smaller than 31 nm and specific surface area between 37 and 57 $m^2 \bullet g^{-1}$. The best photocatalytic activity for H_2 production was obtained on α-Fe_2O_3 calcined at 500°C, with an average evolution rate of 0.015 $cm^3 \bullet h^{-1} \bullet (mg\ catalyst)^{-1}$.

Solvothermal methodology is a versatile process to synthesize uniform-sized nanoparticles, which are formed from iron salts dissolved in non-aqueous solvents, usually alcohol. This mixture often is transferred to autoclave to achieve reaction temperature near 180°C [38, 43]. Preparation of hematite nanoparticles through alcoholysis of ferric chloride under solvothermal condition has been carried out by [48]. $FeCl_3 \bullet 6H_2O$ was dissolved in ethanol and transferred into Teflon autoclave to achieve 180°C. This synthetic method applied created core/shell structures formed from α-Fe_2O_3 nanoparticles, which were used as catalysts in the oxidation of benzyl alcohol to benzaldehyde with 42% conversion and 95% selectivity. Sun et al. [49] developed a combined solvothermal/microwave method to prepare α-Fe_2O_3 nanosheet-assembled hierarchical hollow mesoporous microspheres from chloride ferric precursors dissolved in ethylene glycol. The reaction occurred into autoclave at 180°C for 180 min and the nanoparticles formed were applied to salicylic acid degradation, with removal efficiencies near 50%.

Hydrothermal is the most applied process in the synthesis of hematite due to low cost and energy consumption, high purity and short time to preparation. In this method, the iron (III) chloride or nitrate solutions are dispersed in aqueous media that contains ammonia to adjust the pH value above 9.0. Later, the solution is heated at high temperatures (≈ 150°C) in an autoclave to decompose the precursors and combine their ions to form new compounds with high homogeneity [50, 51]. Hematite nanoparticles were synthesized by [52] by a simple hydrothermal synthesis method using only $Fe(NO_3)_3 \bullet 9H_2O$ and $NH_3 \bullet H_2O$ as raw materials into a Teflon autoclave at different temperatures (80, 100, 120 and 150°C) for 10 h. This research demonstrated that nanoparticles with diameter of 30–100 nm only were produced at temperatures above 120°C in a reaction time within 5 h, occurring an increase in the particles size when longer times were evaluated. The methylene blue adsorption on surface of nanostructured t-ZrO2-modified α-Fe_2O_3 composite synthesized in a mesoporous structure by a hydrothermal route was studied by [53]. The composite was prepared from $FeCl_3 \bullet 6H_2O$ and $ZrOCl_2 \bullet 8H_2O$ dissolved in an aqueous media with cetyl trimethyl ammonium bromide (CTAB). Thereafter, the reaction mixture was transferred to a Teflon autoclave and heated at 180°C for 48 h. The

nanoparticles synthesized showed excellent adsorption capacity with an efficient upper 95% in the removal of chromium, cobalt, nickel, cadmium, lead, copper and mercury. Dong et al. [54] obtained grain-like hematite by hydrothermal approach using $FeCl_3 \bullet 6H_2O$ and urea dissolved in a water-ethanol solution heated at 180°C for 8 h in a Teflon autoclave. The researchers determined that in a volume ratio of ethanol/water equal to 1:1, the grain-like nanoparticle formation is favored, with no regular structures, when only water or alcohol were used. The photocatalyst response achieved approximately 99% of dye removal after 24 h under visible light.

The researches above-mentioned investigated the adsorption capacity and photocatalysis separately, however the hematite is interesting to organic and inorganic compound removal in water due to the join between both systems, since this photocatalytic adsorbent has a system that captures and degrades the contaminants efficiently. The conjugated response of hematite was evaluated by [55] that synthesized nanoparticles with 75 nm and a specific surface area near 25 $m^2 \bullet g^{-1}$, which showed a high adsorption capacity (84 $mg \bullet g^{-1}$) and limited photocatalytic degradation ($\approx$ 20%).

Cheng et al. [56] also analyze the conjugated adsorption and photocatalytic removal of organic dye rhodamine B for cauliflower-like α-Fe_2O_3 microstructures constructed by nanoparticle-based buds. The hematite nanoparticles were synthesized from aqueous solution containing ammonia and polyvinylpyrrolidone (PVP) that was mixed with Fe(acetylacetonate)$_3$ dispersed in a toluene solution and transferred to autoclave at 150°C for 24 h. The structure formed with high surface area (31.57 $m^2 \bullet g^{-1}$) were shown to exhibit adsorption efficient near 80% of organic dye in wastewater and structurally enhanced visible light photocatalytic activity, with a degradation above 90% in the presence of H_2O_2.

Liu et al. [57] prepared α-Fe_2O_3 hollow spheres with novel multiple porous shells by solvothermal treatment of $FeCl_3 \bullet 6H_2O$ dissolved in ethylene glycol and CH_3COONa. Carbon spheres were added into the mixture and the resultant suspension was transferred to an autoclave at 200°C for 10 h. The carbon was removed by calcination at 500°C during 3 h. The nanostructures formed are composed of particles from 20 to 40 nm in size that reduced the dye concentration below 90% due to the synergistic effect of adsorption and photocatalysis.

Hematite nanoparticles were synthesized by [58] applying hydrothermal method to react $FeCl_3 \cdot 6H_2O$ dissolved in aqueous solution containing NH_4OH and pectin into a Teflon autoclave. The size of the nanoparticles was achieved as 42 nm when pectin was added probably due to less agglomeration. The experimental data demonstrated that dye removal reached values upper 80% when only adsorption was applied, as well as when the photocatalysis is incorporated.

3. Metal-organic frameworks (MOFs)

Metal-organic frameworks (MOFs) are a class of functional materials synthesized by the assembly of the metal ions/clusters and organic linkers like cyano and pyridyl, carboxylates, phosphonates and crown ethers, which are connected to metal ions/clusters through coordination bonds of moderate strength [59, 60]. The MOFs have been studied since 1990s with more than 20,000 structures synthesized and evaluated for applications such as adsorption, catalysis, drug delivery, sensing, separation, gas storage, bioimaging and so on [61–64]. These structures have shown huge potential in these areas due to distinctive features, such as high porosity and surface area, chemically adjustable pore, uniform structures, tunable surface properties (functional groups), good thermal stability, unsaturated metal centers and even the catalytically active organic linkers [65–68]. The most typical metal-organic

frameworks are MIL (Materials of Institute Lavoisier), based on lanthanides or transition metals; UiO (University of Oslo), built up with Zr; MOF-5, composed of Zn; and Cu-BTC, based on Cu [69].

These structures have been applied to adsorption of organic and inorganic contaminants in water and wastewater with better efficiencies when compared with conventional adsorbents, probably due to large surface area (1000–10,000 $m^2 \bullet g^{-1}$); presence of central metal ions, open metal sites, coordinatively unsaturated sites and functional groups on the organic linkers; and easily tunable structure and flexible framework, since it is possible to modify the pores surface [66, 70–72]. The adsorption mechanisms for removal of organic pollutants by MOFs in water mainly include electrostatic, hydrophobic, acid-base π-π interactions and hydrogen bonding [73–75].

MOFs photocatalytic properties are exploited due to high capacity of the organic linkers in absorbing photons, such as antennas to harvest light, which transfer the energy to the metal sites by transition from ligand to metal cluster charge under UV or visible light radiation [76, 77]. Therefore, these structures can act as semiconductor, since MOFs contain conduction and valence bands, with band gaps in the range of 1.0–5.5 eV, or the band gaps are related to the energy levels of the highest occupied molecular orbitals (HOMOs) and lowest unoccupied molecular orbitals (LUMOs) of the linker molecules, which leads to the formation of charge carriers (e^-/h^+) that can subsequently be transferred to the surface [60, 68]. Furthermore, the easily tailorable physical and chemical functions, together with the large surface area and permanent pores/channels to potentially anchor/encapsulate photosensitizers and catalytic moieties, make MOFs potential candidates for application in photocatalytic processes [78].

The photocatalytic and adsorption features of the metal-organic frameworks are directly related to synthetic routes and parameters such as temperature, reagent concentration, solvent, pH and pressure [79]. Many techniques have been studied to produce distinct structures with specific properties, such as hydro/solvothermal, electrochemical, mechanochemical and solvothermal [80–82].

Electrochemical method to synthesize MOFs is based on the dissolution of a anodic metal that supply metal ions into a reaction medium that contains the organic linkers and electrolytes, avoiding the use of metal salts. This reaction between metal ions and organic linkers produces structures with high purity, due to the absence of nitrate, perchlorate or chloride presents in metal salts, in a short time when compared to other synthetic methods [83–85]. The electrochemical approach was applied by [86] to produce $Cu_3(BTC)_2$ (HKUST-1) for CO_2 and CH_4 adsorption and separation. Two copper electrodes were used into a solution that contained benzene-1,3,5-tricarboxylate (H_3BTC) and tetrabutylammonium tetrafluoroborate (TBAFB) as electrolytes to form the MOF. The characterization confirmed the high textural properties, high crystallinity and good thermal stability of the structure, which showed satisfactory CO_2 adsorption. A microseparator device containing a metal-organic framework synthesized by electrochemical method was produced by [87]. HKUST-1 was prepared by copper electrodes, benzene-1,3,5-tricarboxylate (BTC) linker and methyl-tributyl-ammonium methyl sulfate (MTMS) electrolyte and was applied to the separation of methanol and n-hexane. The breakthrough curves analysis demonstrated that up to 400 $mg \bullet g^{-1}$ of methanol can be adsorbed to the electrochemically synthesized Cu-BTC coating. Yang et al. [88] synthesized MOF-5 using zinc anodes, terephthalic acid (H_2BDC) linker, zinc nitrate hexahydrate [$Zn(NO_3)_2 \cdot 6H_2O$] electrolyte and 1-butyl-3-methylimidazolium chloride ionic liquid, which was employed to a template to induce the porous structure. This structure was mixed with BiOBr by ultrasound treatment to create a composite that was evaluated for methyl orange dye degradation by photocatalysis under simulated solar light irradiation. The results showed that this new composite can achieve degradation more than 90% that occurs mainly because of the H^+ and $\bullet O_2^-$ active species.

Mechanochemical method is a solvent free methodology to produce MOFs that employ a direct mechanical grinding of the metal salts and linker precursors either in a mortar or a ball mill [89]. This technique can occur at room temperature in short reaction times [90]. The compound MOF-14 [$Cu_3(BTB)_2$] was synthesized by [91] using ball milling to copper acetate monohydrate (metal salt) and H_3BTB (organic linker) mixture, which were placed in a ball mill with three balls and grinded together for 10 min and later activated by a single post-synthetic washing step with ethanol. This structures showed high micropore volume and a specific surface area near 1200 $m^2 \bullet g^{-1}$. Framework $Zn_2(oba)_2(4\text{-bpdb}) \cdot (DMF)_x$ (TMU-4) and $Zn_2(oba)_2(4\text{-bpdh}) \cdot (DMF)_y$ (TMU-5) were prepared by mechanochemical by [92] from a mixture of 4,4′-oxybisbenzoic acid (H_2oba) and 1,4-bis(4-pyridyl)-2,3-diaza-1,3-butadiene (4-bpdb) or 2,5-bis(4-pyridyl)-3,4-diaza-2,4-hexadiene (4-bpdh), respectively, for 15 min. The structures obtained possess different structural topologies, metal-ligand connectivities and therefore different pore sizes. Furthermore, the pore surface in both networks were capable to capture CO_2, achieving 60 $cm^3 \bullet g^1$. Chen et al. [93] synthesized $In_2(OH)_2(BPTC)] \cdot 6H_2O$ (InOF-1) by mechanochemical route from indium acetate hexahydrate $In(OAc)_3 \cdot 6H_2O$ and organic linker 3,3′,5,5′-biphenyltetracarboxylic acid (H_4bptc), which were filled in a stainless steel milling jar for different times (10–60 min). InOF-1 showed moderate adsorption capacity for CO_2 and high for CO_2/CH_4 and CO_2/N_2 adsorption selectivities.

In the sonochemical technique, the MOF synthesis occurs due to extremely high temperature (≈ 4000 K) and pressure (≈ 1000 atm) in microenvironment formed by acoustic cavitation generated by ultrasound, which starts the chemical bonds breakage of the elements in the solution and allows interaction between metal salts and organic linkers [94, 95]. This is an environment friendly method to produce homogeneous nucleation centers in a short time and with low energy consumption [79]. Zn(II)-based metal-organic framework $[Zn(TDC)(4\text{-BPMH})]_n \cdot n(H_2O)$ was produced by [96] from 2,5-thiophene dicarboxylic acid (TDC) linker, N,N-bis-pyridin-4-ylmethylene-hydrazine (4-BPMH) as pillar spacer and zinc nitrate hexahydrate $[Zn(NO_3)_2 \cdot 6H_2O)$ as metal precursor. The MOFs nanoparticles were sonochemically synthesized under atmospheric pressure using an ultrasonic bath with different irradiation powers, irradiation time, precursor concentrations and temperatures. Adsorption capacities of 2,4-dichlorophenol and amoxicillin were evaluated in aqueous media and their related results demonstrated an efficiency nearly 90% for both cases. Sonochemical method was employed by [97] to synthesize $[Cd(oba)(4\text{-bpdh})]_n \bullet 1DMF$ (TMU-7) using the ligand 4,4-oxybisbenzoic acid (H_2oba), the N-donor ligand 2,5-bis(4-pyridyl)-3,4-diaza-2,4-hexadiene (4-bpdh) and the metal precursor zinc acetate tetrahydrate [Zn(OAc)2•$4H_2O$]. Synthesis of TMU-7 was carried out in an ultrasonic bath at ambient temperature and atmospheric pressure with different reaction times and concentrations of metal and ligands to evaluate the morphology. The results showed that the Congo red dye was efficiently removed when this nanostructures were used, achieving an adsorption approximately equal 97%. Abdollahi et al. [98] produced $Zn_4(oba)_3(DMF)_2$ from $Zn(NO_3)_2 \cdot 6H_2O$ and H_2oba dispersed in DMF. MOFs syntheses were carried out in an ultrasonic bath at ambient temperature and atmospheric pressure for different reaction times and concentrations of initial precursors. In comparison of samples synthesized by solvothermal and sonochemical methods, the nanostructures synthesized by ultrasound have been more efficient to remove Congo red and Sudan red dyes, with an adsorption efficiency approximately 53 and 87%, respectively.

Hydro/solvothermal synthesis is the most classical route to produce metal-organic frameworks nanoparticles. This method involves the heterogeneous reaction between organic linkers and metal salts that are dissolved in water or organic solvents (e.g. alcohols and pyridine) under moderate to high temperatures

and pressures [84]. This reaction occurs in sealed reactor vessels (autoclave) under conditions above the boiling point of the solvent and usually takes place over days or hours [99, 100]. The frameworks synthesized by hydro/solvothermal synthesis are nanoparticles with high crystallinity and good size control, which are insoluble in the solvent [70]. Mn (II) ions based metal-organic framework was synthesized by solvothermal method described in [101]. A solution of 1,3,5-tris(4-carboxyphenyl) benzene acid (H_3BTB) as linker, manganese (II) acetate [$Mn(OAc)_2$] as metal salt, imidazole and d L-N-tert-butoxycarbonyl-2-(imidazole)-1-pyrrolidine (L-BCIP) as chiral adduct were sealed in a Teflon stainless steel vessel at 110°C for 3 days. The adsorption rate for methylene blue was nearly 90% after 120 min, when the MOF was used. The zinc-based MOF ($[Zn_5(FODC)_2(OCH_2CH_2O)_3(H_2O)]\bullet(sol)_n$) was synthesized by solvothermal method [102] and evaluated for adsorption and selective separation of methylene blue (MB), crystal violet (CV) and rhodamine B (RhB). Fluorenone-2,7-dicarboxylate (H_2FODC) ligand and $Zn(OAc)_2\bullet4H_2O$ were mixed and transferred to stainless steel reactor with a Teflon stainless steel autoclave, sealed and heated up to 110°C for 3 days. The structures produced showed high affinity to cationic dyes, with removal rates of MB, CV and RhB on the Zn-MOF equal to 98.44, 90.77 and 41.99%, respectively. The photocatalytic response of $[Ni(azp)(ppa)(H_2O)_2]_n$ metal-organic framework was studied by [103]. This structure was produced from the salt metal nickel nitrate hexahydrate ($[Ni(NO_3)_2]\bullet6H_2O$), the O-donor ligand 1,4-phenylenedipropionic acid (PPA) and four N,N′-donors ligands [4,4′-azodipyridine (AZP); 4,4′-trimethylenedipyridine (TMDP); 1,2-bis-(4-pyridyl)ethane (BPETHA) and 4,4′-bipyridine (BPY)]. The solutions were individually placed in a Teflon-lined stainless steel heated at 80°C for 10 h and then continuously heated at 120°C for 24 h. The new structures formed displayed diverse structural architectures due to a variety of the length and flexibility of N,N′-donors ligands and the varied coordination modes of PPA. The band gaps of the MOFs were between 3.3 and 3.7 eV, with a photocatalytic degradation of MB roughly in the range of 65–97%. Gao et al. [104] evaluated the photocatalytic degradation of Acid Orange 7 dye in aqueous solution over MIL-53(Fe) under visible LED light irradiation and in the presence of persulfate oxidant. The framework was synthesized by solvothermal technique from a mixture of $FeCl_3{\cdot}6H_2O$, 1,4-benzenedicarboxylic acid (H_2BDC) organic linker and DMF. The reactant mixture was transferred into a Teflon-lined stainless steel autoclave and heated at 150°C for 15 h. MIL-53(Fe) band gap was determined equal to 2.62 eV and the photocatalytic degradation response demonstrated that this structure can degrade Acid Orange 7 via the direct hole oxidation pathway under visible light, achieving a removal efficiency upper 90% after 90 min.

Nevertheless, such as above mentioned, for the removal and degradation processes is interesting the evaluation of adsorption and photocatalytic effects coupled. In this context, Gao et al. [105] evaluated the adsorption and visible light photodegradation of aqueous clofibric acid (CA) and carbamazepine (CBZ) by MIL-53(Fe) metal-organic framework prepared by solvothermal method. MOF synthesis was performed from a mixture of $FeCl_3\bullet6H_2O$, terephthalic acid and DMF that was introduced in a Teflon-lined steel autoclave and maintained at 120°C for 3 days. The adsorption and photocatalytic experiments evaluated the pH effect and the related results suggested that the adsorption of CA and CBZ were mainly ascribed to electrostatic interactions and π–π interactions, respectively. In pH equal 3.0, the maximum adsorption capacity of CA and CBZ on MIL-53(Fe) were 0.80 and 0.57 $mmol\bullet g^{-1}$, respectively, and the photodegradation efficiency for CA and CBZ was greater than 90%, when H_2O_2 was used as oxidant.

Araya et al. [106] synthesized the FeBTC MOF modified with Amberlite IRA-200 resin to yield a novel heterogeneous photocatalyst, A@FeBTC, to degrade

Rhodamine B dye. The iron-based framework was synthesized using the hydrothermal method from H_3BTC, iron powder, hydrofluoric acid, nitric acid and water. The reaction mixture was transferred to a Teflon-lined pressure vessel and maintained at 160°C for 12 h. A@FeBTC catalyst was prepared by grinding and stirring the powdered resin in an aqueous suspension of FeBTC for 24 h, with different resin/FeBTC mass ratio. All samples (with or without Amberlit resin) were evaluated to dye removal and showed adsorption efficiency greater than 20% and photodegradation responses upper 95% for A@FeBTC and FeBTC.

Simultaneously efficient adsorption and photocatalytic degradation of tetracycline by Fe-MIL-101, Fe-MIL-100 and Fe-MIL-53 was studied by [107]. MOFs were synthesized by a hydrothermal method from $FeCl_3$•$6H_2O$ and H_2BDC dissolved in DMF. The solution was sonicated, transferred to a Teflon-lined stainless steel autoclave and maintained at 110°C in an oven for 20 h for Fe-MIL-101 and maintained at 150°C for 12 h for Fe-MIL-53. In the synthesis of Fe-MIL-100, a mixture of $FeCl_3$•$6H_2O$, H_2BDC and hydrofluoric acid was dissolved in DMF and magnetically stirred. The solution was heated at 160°C for 12 h into a Teflon-lined stainless steel autoclave. The effects of adding dosage and initial concentration of tetracycline on degradation efficiency were examined and the results revealed that a Fe-MIL-101 catalyst dosage equal 0.5 g•l^{-1} showed the best photocatalytic efficiency. Tetracycline was efficiently adsorbed and degraded by Fe-MIL-101, reaching approximately 55% only by adsorption removal and 96.6% after photocalysis process.

Abdpour et al. [108] evaluated the MIL-100(Fe)@MIL-53(Fe) photocatalytic performance of methyl orange degradation under visible light. Firstly, MIL-100(Fe) was synthesized by solvothermal method from H_2BTC and $FeCl_3$·$6H_2O$ dissolved in distilled water in the presence of HNO_3 and HF. The resulted solution was stirred, transferred to the autoclave and heated at 150°C for 20 h. Then, different amounts of MIL-100(Fe) nanoparticles were dispersed in DMF by ultrasonication. $FeCl_3$.$6H_2O$ and H_2BDC were added in this solution, which was stirred and placed in the ultrasonic generator probe for 15 min at 50% of the maximum power. The sonochemically synthesized the metal-organic framework was denominated MIL-100(Fe)@MIL-53(Fe). The band gaps energies calculated for the samples were around 2.5 eV. The results showed that all samples reached adsorption efficiencies near 10–15%, whereas the samples that contained 0.03 and 0.04 g of MIL-100(Fe) achieved the highest photocatalytic degradation (≈70%). The reduction of the photogenerated electron-hole pairs recombination probably occurs due to the decrease in photoluminescence intensity because excited electron transfer from the conduction band of MIL-100(Fe) to MIL-53(Fe) and hole transfer from the valance band of MIL-53(Fe) to MIL-100(Fe), which prolong the lifetime of the separated electrons and holes in the MIL-100(Fe)@MIL-53(Fe).

4. α-Fe_2O_3@TiO_2, MOF@TiO_2 and others TiO_2 nanocomposites

TiO_2 application as a photocatalyst is of great interest because this compound is nontoxic, economically viable, chemically inert, photostable to corrosion, besides having high thermal stability and intense photocatalytic activity and oxidation power [22, 109]. The main crystalline structures of titanium dioxide are anatase, rutile and brookite, but the last one is difficult to be synthesized in laboratory [110]. However, not all crystalline structures have the same efficiency in the absorption of light for catalysis, and rutile, although the polymorph thermodynamically more stable has reduced photocatalytic activity in comparison to anatase [111]. This occurs possibly due to the high temperature required for its preparation, resulting in an increase in the particle size, lower electron mobility in relation to anatase

and high rate of electron/vacancy recombination, that cause a reduced number of hydroxyl groups on the surface [10].

However, despite all these favorable features, TiO_2 has some limitations that affects its large-scale application in industrial processes, such as the recombination of photogenerated charges due to defects, impurities or other imperfections on crystal surface, which reduce the photocatalytic efficiency. In addition, the band gap energy required for the formation of the electron/vacancy pair is equal to 3.2 eV, which restricts this catalyst to the use of UV-light [112]. Since only 5% of sunlight wavelengths are in the UV region, an alternative energy source is necessary, making the process more expensive when this semiconductor is applied [23]. Furthermore, the reactive oxygen species (ROS) are formed on the surface of the titanium dioxide, mainly due to the reaction and capture of an electron of the water molecule by the vacancy present on this surface or by the electron donation on the CB. Accordingly, the higher density of radicals is close to the semiconductor surface. Therefore, strategies that improve the incidence of the molecules on the surface of the photocatalyst, like adsorption, would increase the probability of attack and degradation of these molecules by ROS. This can enhance the selectivity and the photocatalytic capacity of this advanced oxidation process.

Therefore, many efforts have been performed to improve the adsorption capacity and photocatalytic efficiency of TiO_2. Structural modifications of TiO_2 have been proposed to improve the photocatalysis, such as metal deposition, doping with nonmetals, functionalization with organic molecules or coupling of other metals with TiO_2 [25, 113]. Different methods have been adopted to synthesize TiO_2 nanoparticles such as sol-gel, solvothermal, hydrothermal, sonochemical and mechanochemical, which were described in the above sections [114–116].

Cheng et al. [117] synthesized a Fe_2O_3@TiO_2 nanocomposite with high adsorption and photocatalytic activity by solvothermal method. Titanium glycolate precursor and $(NH_4)_2Fe(SO_4)_2{\bullet}6H_2O$ were dispersed by vigorous sonication in deionized water. This reaction mixture was autoclaved for 6 h at 180°C in a Teflon-lined autoclave. The combined effect of adsorption and photocatalysis were evaluated by Rhodamine B degradation under visible light. It was observed that the TiO_2@Fe_2O_3 exhibited improved adsorption (RhB removal ≈ 20%) and photocatalytic (RhB degradation ≈ 75%) capability compared to pure TiO_2 and Fe_2O_3 nanoparticles.

Fe_2O_3@TiO_2 nanocomposite was prepared via mechanochemical process by [118]. Commercial P25® and different amounts of magnetic Fe_3O_4 nanoparticles were mixed by a mechanical process and the mixtures were calcined at 450°C for 2 h. XRD characterizations revealed that the samples are formed basically for TiO_2 and α-Fe_2O_3 after calcination, with high purity. MB adsorption efficiency is near 15% for 5%-$Fe_2O_32TiO_2$ with photocatalytic degradation approximately equal to 65% after 80 min under visible light.

TiO_2@MIL-101 core-shell structure was synthesized by [119] under hydrothermal method and investigated for adsorption and photocatalytic degradation of methyl orange. MIL-101 was synthesized under hydrothermal conditions and added with titanium butoxide into ethanol solution under stirring. Then, ultrapure water was added into the solution that was transferred into a Teflon-lined bomb sealed and heated at 220°C for 3 h to produce TiO_2@MIL-101 core-shell composites. The results revealed that the TiO_2@-MIL-101 core-shell composite possessed excellent adsorption of MO (removal ≈ 70%), probably due to π-π interaction between benzene rings in MO and MIL-101, and also showed inspiring property on the degradation of MO, reaching a removal efficiency equal 97% after 50 min under UV-light radiation.

A photocatalytic adsorbent, N-doped TiO_2 nanoparticles encapsulated in MIL-100(Fe) cages was developed by [120] for the adsorption and photocatalytic

degradation, enhances methylene blue (MB) and rhodamine B (RhB) under visible light. MIL-100(Fe) was synthesized under hydrothermal technique from a mixture of Fe powder, H_3BTC, HF, HNO_3 and H_2O that was stirred and transferred into a Teflon-lined stainless steel autoclave at 150°C for 12 h. The samples of MIL-100(Fe) encapsulating N-TiO_2 nanoparticles were prepared by impregnating MIL-100(Fe) in a dilute suspension that contained different concentrations of as-prepared neutral N-TiO2 nanoparticles. This mixture was stirred for 3 h at ambient temperature, dried and calcinated at 150°C for 4 h. All the samples showed adsorption efficiencies greater than 80% under dark conditions, probably related to MOFs pore size (≈1.93 nm) and high surface area (≈1400 $m^2 \bullet g^{-1}$). The photocatalytic activity of 32%N-TiO_2@MIL-100(Fe) sample was the highest of all samples evaluated, with an degradation efficiency equal 99.1% for MB and 93.5% for RhB.

However, to improve the adsorption capacity and to enhance the photocatalytic capacity, researchers have evaluated the inclusion of distinct organic and inorganic compounds, such as cyclodextrins and their derivatives, noble metals (silver), lanthanides (cerium, samarium, lanthanum and neodymium), graphene, zeolites, alumina and silica.

In this context, Dal'Toé et al. [121] investigated the incorporation of plasmonic Ag nanoparticles on the physicochemical and photocatalytic properties of La-doped TiO_2 nanostructure. The nanocrystalline La-doped TiO_2 powder was prepared by an ultrasound-assisted wet impregnation method. $La(NO_3)_3 \bullet 6H_2O$ and commercial TiO_2 P25® were dispersed in distilled water and stirred for 30 min. Then, the solution was ultrasonically processed for 3 h. After the ultrasound processing, the solution was heated to the boiling point and left evaporating for 40 min. The as-obtained paste was dried overnight at 120°C. The resultant solid was ground with a pestle to obtain a fine powder, which was calcined at 500°C for 1 h. Then, La/TiO_2 sample was dispersed into distilled water and aliquots of $AgNO_3$ solution was added according to the desired Ag molar ratio (0.5–5%). The mixture was then photoirradiated under 80 W Hg vapor lamp and dried. The results revealed an increase in the adsorption capacity of the nanoparticles when the Ag molar ratio is between 2 and 4%, with efficiencies more than 65%, which proportionally increased the photocatalytic activity. Thus, the enhancements achieved in the photocatalytic decolorization (>95% in 30 min) of MB by Ag-La/TiO_2 materials are directly related to the increased adsorption capacity.

On the other hand, organic molecules functionalization to enhance the photocatalytic activity of TiO_2 was proposed by [122]. Carboxymethyl-β-cyclodextrin (CMCD) functionalization of TiO_2 doped with lanthanum was evaluated to MB adsorption and degradation under UV-light radiation. TiO_2-La nanoparticles were synthesized as described by [121]. The CMCD was synthesized by the dissolution of β-CD and NaOH aqueous $ClCH_2COOH$ solution, which was maintained at 50°C in a jacketed reactor for 5 h. A white precipitate (CMCD) was obtained by addition of methanol and acetone to the solution. The CMCD functionalized catalysts were prepared TiO_2–La dispersed in distilled water. This solution was added to CMCD along with cyanamide and maintained at 90°C for 4 h. The results showed that adsorption efficiency increase for CMCD@TiO_2-La sample, with a removal near 15% after 60 min under dark conditions. Accordingly, the improvement of the photocatalytic activity achieved for this nanoparticle is also related to the adsorption of the MB by CMCD, although the mass transfer is low due to the reduced concentration of this oligosaccharide at the TiO_2 nanoparticles surface. This increase in degradation efficiency occurs because the CMCD has the function of enhancing the density of the dye at the semiconductor and solution interface, where the ROS are formed. Usually these species return to a thermodynamically

stable state without reacting with organic molecules due to their short lifetimes and because the contaminants are dispersed in the solution. Thus, when the dye is adsorbed, the transfer of electrons between the ROS and the contaminant becomes more probable, increasing the efficiency of the process.

5. Conclusions

Photocatalytic adsorbents nanoparticles have a tremendous potential to wastewater treatment for capture and degrade many contaminants. Coupling of adsorption and photocatalysis demonstrated to be an efficient process to overcome of the limitations presented by the separated techniques. α-Hematite and metal-organic frameworks have exhibited excellent adsorption performance for removing contaminants from aqueous solutions and superior photocatalytic capacities to degrade and mineralize many recalcitrant compounds in visible light. Some researches have been developed to couple the TiO_2 properties with MOFs or α-Fe_2O_3, as well as other inorganic or organic compounds, to enhance the photocatalytic activity. As illustrated in this review, a range of photocatalytic adsorbents technologies have been proposed or are under active development for wastewater treatment, but many techniques are still at an experimental or pilot stage.

Acknowledgements

The authors acknowledge the Community University of Chapecó and Region (Unochapecó), for technical and scientific support.

Conflict of interest

There are no conflicts to declare.

DOI: http://dx.doi.org/10.5772/intechopen.79954

Author details

Gustavo Lopes Colpani[1], Adrieli Teresinha Odorcik Dal'Toé[2], Micheli Zanetti[3], Rubieli Carla Frezza Zeferino[3], Luciano Luiz Silva[1], Josiane Maria Muneron de Mello[1,4] and Márcio Antônio Fiori[1,4]*

1 Post-Graduation Program in Management and Innovation Technology (PPGTI)—Unochapecó, Chapecó, Brazil

2 Federal University of Santa Catarina—UFSC, Florianópolis, Brazil

3 Chemical and Food Engineering—Unochapecó, Chapecó, Brazil

4 Post-Graduation Program in Environment Science (PPGCA)—Unochapecó, Chapecó, Brazil

*Address all correspondence to: fiori@unochapeco.edu.br

References

[1] Matamoros V, Rodríguez Y, Albaigés J. A comparative assessment of intensive and extensive wastewater treatment technologies for removing emerging contaminants in small communities. Water Research. 2016;**88**:777-785. DOI: 10.1016/j.watres.2015.10.058

[2] Yuan J, Dyke MI, Huck PM. Identification of critical contaminants in wastewater effluent for managed aquifer recharge. Chemosphere. 2017;**172**:294-301. DOI: 10.1016/j.chemosphere.2016.12.120

[3] Naidu R, Espana VAA, Liu Y, Jit J. Emerging contaminants in the environment: Risk-based analysis for better management. Chemosphere. 2016;**154**:350-357. DOI: 10.1016/j.chemosphere.2016.03.068

[4] Noguera-Oviedo K, Aga DS. Lessons learned from more than two decades of research on emerging contaminants in the environment. Journal of Hazardous Materials. 2016;**316**:242-251. DOI: 10.1016/j.jhazmat.2016.04.058

[5] Petrie B, Barden R, Kasprzyk-Hordern B. A review on emerging contaminants in wastewaters and the environment: Current knowledge, understudied areas and recommendations for future monitoring. Water Research. 2015;**72**:3-27. DOI: 10.1016/j.watres.2014.08.053

[6] Malato S, Ibáñez PF, Maldonado MI, Blanco J, Gernjak W. Decontamination and disinfection of water by solar photocatalysis: Recent overview and trends. Catalysis Today. 2009;**147**:1-59. DOI: 10.1016/j.cattod.2009.06.018

[7] Kaur A, Umar A, Kansal SK. Heterogeneous photocatalytic studies of analgesic and non-steroidalanti-inflammatory drugs. Applied Catalysis A: General. 2016;**510**:134-155. DOI: 10.1016/j.apcata.2015.11.008

[8] Ribeiro AR, Nunes OC, Pereira MFR, Silva AMT. An overview on the advanced oxidation processes applied for the treatment of water pollutants defined in the recently launched Directive 2013/39/EU. Environmental International. 2015;**75**:33-51. DOI: 10.1016/j.envint.2014.10.027

[9] Teh CM, Mohamed AR. Roles of titanium dioxide and ion-doped titanium dioxide on photocatalytic degradation of organic pollutants (phenolic compounds and dyes) in aqueous solutions: A review. Journal of Alloys and Compounds. 2011;**509**:1648-1660. DOI: 10.1016/j.jallcom.2010.10.181

[10] Zangeneh H, Zinatizadeh AAL, Habibi M, Akia M, Isa MH. Photocatalytic oxidation of organic dyes and pollutants in wastewater using different modified titanium dioxides: A comparative review. Journal of Industrial and Engineering Chemistry. 2015;**26**:1-36. DOI: 10.1016/j.jiec.2014.10.043

[11] Nazari G, Abolghasemi H, Esmaieli M, Pouya ES. Aqueous phase adsorption of cephalexin by walnut shell-based activated carbon: A fixed-bed column study. Applied Surface Science. 2016;**375**:144-153. DOI: 10.1016/j.apsusc.2016.03.096

[12] Song JY, Bhadra BN, Jhung SH. Contribution of H-bond in adsorptive removal of pharmaceutical and personal care products from water using oxidized activated carbon. Microporous and Mesoporous Materials. 2017;**243**:221-228. DOI: 10.1016/j.micromeso.2017.02.024

[13] Darweesh TM, Ahmed MJ. Adsorption of ciprofloxacin and norfloxacin from aqueous solution onto granular activated carbon in fixed bed column. Ecotoxicology and

Environmental Safety. 2017;**138**:139-145. DOI: 10.1016/j.ecoenv.2016.12.032

[14] Fayazi M, Ghanei-Motlagh M, Taher MA. The adsorption of basic dye (alizarin red S) from aqueous solution onto activated carbon/γ-Fe_2O_3 nano-composite: Kinetic and equilibrium studies. Materials Science in Semiconductor Processing. 2015;**40**: 35-43. DOI: 10.1016/j.mssp.2015.06.044

[15] Kim Y, Bae J, Park J, Suh J, Lee S, Park H, et al. Removal of 12 selected pharmaceuticals by granular mesoporous silica SBA-15 in aqueous phase. Chemical Engineering Journal. 2014;**256**:475-485. DOI: 10.1016/j.cej.2014.06.100

[16] Mehrjouei M, Müller S, Möller D. A review on photocatalytic ozonation used for the treatment of water and wastewater. Chemical Engineering Journal. 2015;**263**:209-219. DOI: 10.1016/j.cej.2014.10.112

[17] Kanakarajua D, Kockler J, Motti CA, Glass BD, Oelgemöller M. Titanium dioxide/zeolite integrated photocatalytic adsorbents for the degradation of amoxicillin. Applied Catalysis B: Environmental. 2015;**166-167**:45-55. DOI: 10.1016/j.apcatb.2014.11.001

[18] Cheng M, Zeng G, Huang D, Lai C, Xu P, Zhang C, et al. Hydroxyl radicals based advanced oxidation processes (AOPs) for remediation of soils contaminated with organic compounds: A review. Chemical Engineering Journal. 2016;**284**:582-598. DOI: 10.1016/j.cej.2015.09.001

[19] Wng N, Zheng T, Zhang G, Wang P. A review on Fenton-like processes for organic wastewater treatment. Journal of Environmental Chemical Engineering. 2016;**4**:762-787. DOI: 10.1016/j.jece.2015.12.016

[20] Reddy PVL, Kim KH. A review of photochemical approaches for the treatment of a wide range of pesticides. Journal of Hazardous Materials. 2015;**285**:325-335. DOI: 10.1016/j.jhazmat.2014.11.036

[21] Coronado JM, Fresno F, Hernández-Alonso MD, Portela R. Design of advanced photocatalytic materials for energy and environmental applications. In: Green Energy and Technology. 1st ed. London: Springer-Verlag; 2013. 351 p. DOI: 10.1007/978-1-4471-5061-9_1

[22] GAYA UI. Heterogeneous Photocatalysis Using Inorganic Semiconductor Solids. 1st ed. Dordrecht: Springer Science + Business Media; 2014. 222 p. DOI: 10.1007/978-94-007-7775-0

[23] Zhao C, Pelaez M, Dionysiou DD, Pillai SC, Byrne JA, O'shea KE. UV and visible light activated TiO_2 photocatalysis of 6-hydroxymethyluracil, a model compound for the potent cyanotoxin cylindrospermopsin. Catalysis Today. 2014;**224**:70-76. DOI: 10.1016/j.cattod.2013.09.042

[24] Spasiano D, Marotta R, Malato S, Fernandez-Ibañez P, Somma I. Solar photocatalysis: Materials, reactors, some commercial, and pre-industrialized applications. A comprehensive approach. Applied Catalysis B: Environmental. 2015;**170-171**:90-123. DOI: 10.1016/j.apcatb.2014.12.050

[25] Wang W, Huang G, Yu JC, Wong PK. Advances in photocatalytic disinfection of bacteria: Development of photocatalysts and mechanisms. Journal of Environmental Science. 2015;**34**: 232-247. DOI: 10.1016/j.jes.2015.05.003

[26] Marschall R, Wang L. Non-metal doping of transition metal oxides for visible-light photocatalysis. Catalysis Today. 2014;**225**:111-135. DOI: 10.1016/j.cattod.2013.10.088

[27] Zhang Q, Lu Z, Jin S, Zheng Y, Ye T, Yang D, et al. TiO_2 nanotube-carbon macroscopic monoliths with multimodal porosity as efficient recyclable photocatalytic adsorbents for water purification. Materials Chemistry and Physics. 2016;**173**:452-459. DOI: 10.1016/j.matchemphys.2016.02.037

[28] Jing HY, Wen T, Fan CM, Gao GQ, Zhong SL, Xu AW. Efficient adsorption/photodegradation of organic pollutants from aqueous systems using Cu_2O nanocrystals as a novel integrated photocatalytic adsorbent. Journal of Materials Chemistry A. 2014;**2**:14563-14570. DOI: 10.1039/c4ta02459a

[29] Mishra M, Chun DM. α-Fe_2O_3 as a photocatalytic material: A review. Applied Catalysis A: General. 2015;**498**:126-141. DOI: 10.1016/j.apcata.2015.03.023

[30] Sajjadia SH, Goharshadi EK. Highly monodispersed hematite cubes for removal of ionic dyes. Journal of Environmental Chemical Engineering. 2017;**5**:1096-1106. DOI: 10.1016/j.jece.2017.01.035

[31] Yuan K, Taylor SD, Powell BA, Becker U. An *ab initio* study of the adsorption of Eu^{3+}, Pu^{3+}, Am^{3+}, and Cm^{3+} hydroxide complexes on hematite (001) surface: Role of magnetism on adsorption. Surface Science. 2017;**664**:120-128. DOI: 10.1016/j.susc.2017.06.007

[32] Noerpel MR, Lenhart JJ. The impact of particle size on the adsorption of citrate to hematite. Journal of Colloid and Interface Science. 2015;**460**:36-46. DOI: 10.1016/j.jcis.2015.08.028

[33] Chen YH, Lin CC. Effect of nano-hematite morphology on photocatalytic activity. Physics and Chemistry of Minerals. 2014;**41**:727-736. DOI: 10.1007/s00269-014-0686-9

[34] Asoufi HM, Al-Antary TM, Awwad AM. Green route for synthesis hematite (α-Fe_2O_3) nanoparticles: Toxicity effect on the green peach aphid, *Myzus persicae* (Sulzer). Environmental Nanotechnology, Monitoring & Management. 2018;**9**:107-111. DOI: 10.1016/j.enmm.2018.01.004

[35] Abu-Dief AM, Abdel-Fatah SM. Development and functionalization of magnetic nanoparticles as powerful and green catalysts for organic synthesis. Beni-Suef University Journal of Basic and Applied Sciences. 2018;**7**:55-67. DOI: 10.1016/j.bjbas.2017.05.008

[36] Kefeni KK, Msagati TAM, Nkambule TTI, Mamba BB. Synthesis and application of hematite nanoparticles for acid mine drainage treatment. Journal of Environmental Chemical Engineering. 2018;**6**:1865-1874. DOI: 10.1016/j.jece.2018.02.037

[37] Mansour H, Bargougui R, Autret-Lambert C, Gadri A, Ammar S. Co-precipitation synthesis and characterization of tin-doped α-Fe_2O_3 nanoparticles with enhanced photocatalytic activities. Journal of Physics and Chemistry of Solids. 2018;**114**:1-7. DOI: 10.1016/j.jpcs.2017.11.013

[38] Fereshteh Z, Salavati-Niasari M. Effect of ligand on particle size and morphology of nanostructures synthesized by thermal decomposition of coordination compounds. Advances in Colloid and Interface Science. 2017;**243**:86-104. DOI: 10.1016/j.cis.2017.03.001

[39] Darezereshki E. One-step synthesis of hematite (α-Fe_2O_3) nano-particles by direct thermal-decomposition of maghemite. Materials Letters. 2011;**65**:642-645. DOI: 10.1016/j.matlet.2010.11.030

[40] Al-Gaashani R, Radiman S, Tabet N, Daud AR. Rapid synthesis and

optical properties of hematite (α-Fe_2O_3) nanostructures using a simple thermal decomposition method. Journal of Alloys and Compounds. 2013;**550**: 395-401. DOI: 10.1016/j.jallcom.2012.10.150

[41] Wang J, Shao X, Zhang Q, Tiana G, Ji X, Bao W. Preparation of mesoporous magnetic Fe_2O_3 nanoparticle and its application for organic dyes removal. Journal of Molecular Liquids. 2017;**248**:13-18. DOI: 10.1016/j.molliq.2017.10.026

[42] Yang X, Xia L, Li J, Dai M, Yang G, Song S. Adsorption of As(III) on porous hematite synthesized from goethite concentrate. Chemosphere. 2017;**169**:188-193. DOI: 10.1016/j.chemosphere.2016.11.061

[43] Nithya VD, Arul NS. Review on α-Fe_2O_3 based negative electrode for high performance supercapacitors. Journal of Power Sources. 2016;**327**:297-318. DOI: 10.1016/j.jpowsour.2016.07.033

[44] Boumaza S, Kabir H, Gharbi I, Belhadi A, Trari M. Preparation and photocatalytic H_2-production on α-Fe_2O_3 prepared by sol-gel. International Journal of Hydrogen Energy. 2018;**43**:3424-3430. DOI: 10.1016/j.ijhydene.2017.07.227

[45] Xiao Q, Sun Y, Zhang J, Li Q. Size-dependent of chromium (VI) adsorption on nano α-Fe_2O_3 surface. Applied Surface Science. 2015;**356**: 18-23. DOI: 10.1016/j.apsusc.2015.08.005

[46] Mathevula LE, Noto LL, Mothudi BM, Chithambo M, Dhlamini MS. Structural and optical properties of sol-gel derived α-Fe_2O_3 nanoparticles. Journal of Luminescence. 2017;**192**: 879-887. DOI: 10.1016/j.jlumin.2017.07.055

[47] Raja K, Jaculine MM, Jose M, Verma S, Prince AAM, Ilangovan K, et al. Sol-gel synthesis and characterization of α-Fe_2O_3 nanoparticles. Superlattices and Microstructures. 2015;**86**:306-312. DOI: 10.1016/j.spmi.2015.07.044

[48] Lian S, Li H, He X, Kang Z, Liu Y, Lee ST. Hematite homogeneous core/shell hierarchical spheres: Surfactant-free solvothermal preparation and their improved catalytic property of selective oxidation. Journal of Solid State Chemistry. 2012;**185**:117-123. DOI: 10.1016/j.jssc.2011.11.003

[49] Sun T, Zhu Y, Qi C, Ding G, Chen F, Wu J. α-Fe_2O_3 nanosheet-assembled hierarchical hollow mesoporous microspheres: Microwave-assisted solvothermal synthesis and application in photocatalysis. Journal of Colloid and Interface Science. 2016;**463**:107-117. DOI: 10.1016/j.jcis.2015.10.038

[50] Bouhjar F, Mollar M, Chourou ML, Marí B, Bessaïs B. Hydrothermal synthesis of nanostructured Cr-doped hematite with enhanced photoelectrochemical activity. Electrochimica Acta. 2018;**260**:838-846. DOI: 10.1016/j.electacta.2017.12.049

[51] Colombo C, Palumbo G, Iorio E, Song X, Jiang Z, Liu Q, et al. Influence of hydrothermal synthesis conditions on size, morphology and colloidal properties of hematite nanoparticles. Nano-Structures & Nano-Objects. 2015;**2**:19-27. DOI: 10.1016/j.nanoso.2015.07.004

[52] Wang F, Qin XF, Meng YF, Guo ZL, Yang LX, Ming YF. Hydrothermal synthesis and characterization of α-Fe_2O_3 nanoparticles. Materials Science in Semiconductor Processing. 2013;**16**:802-806. DOI: 10.1016/j.mssp.2012.12.029

[53] Sengupta A, Mallick S, Bahadur D. Tetragonal nanostructured zirconia modified hematite mesoporous composite for efficient adsorption

of toxic cations from wastewater. Journal of Environmental Chemical Engineering. 2017;**5**:5285-5292. DOI: 10.1016/j.jece.2017.10.002

[54] Dong Y, Xing L, Hu F, Umar A, Wu X. Efficient removal of organic dyes molecules by grain-like α-Fe_2O_3 nanostructures under visible light irradiation. Vacuum. 2018;**150**:35-40. DOI: 10.1016/j.vacuum.2018.01.023

[55] Chen Y, Li F. Kinetic study on removal of copper(II) using goethite and hematite nano-photocatalysts. Journal of Colloid and Interface Science. 2010;**347**:277-281. DOI: 10.1016/j.jcis.2010.03.050

[56] Cheng X, Jiang J, Jin C, Lin C, Zeng Y, Zhang Q. Cauliflower-like α-Fe_2O_3 microstructures: Toluene-water interfaceassisted synthesis, characterization, and applications in wastewater treatment and visible-light photocatalysis. Chemical Engineering Journal. 2014;**236**:139-148. DOI: 10.1016/j.cej.2013.09.089

[57] Liu Y, Yu C, Dai W, Gao X, Qian H, Hua Y, et al. One-pot solvothermal synthesis of multi-shelled α-Fe_2O_3 hollow spheres with enhanced visible-light photocatalytic activity. Journal of Alloys and Compounds. 2013;**551**: 440-443. DOI: 10.1016/j.jallcom.2012.11.047

[58] Rakhshaee R, Darvazeh J. Comparing performance of three forms of hematite in fixed bed reactor for a photocatalytic decolorization: Experimental design, model fitting and optimization of conditions. Process Safety and Environmental Protection. 2017;**107**:122-137. DOI: 10.1016/j.psep.2017.02.006

[59] Mahmoodi NM, Abdi J, Oveisi M, Asli MA, Vossoughi M. Metal-organic framework (MIL-100 (Fe)): Synthesis, detailed photocatalytic dye degradation ability in colored textile wastewater and recycling. Materials Research Bulletin. 2018;**100**:357-366. DOI: 10.1016/j.materresbull.2017.12.033

[60] Shen L, Liang R, Wu L. Strategies for engineering metal-organic frameworks as efficient photocatalysts. Chinese Journal of Catalysis. 2015;**36**:2071-2088. DOI: 10.1016/S1872-2067(15)60984-6

[61] Zhang H, Nai J, Yu L, Lou XWD. Metal-organic-framework-based materials as platforms for renewable energy and environmental applications. Joule. 2017;**1**:77-107. DOI: 10.1016/j.joule.2017.08.008

[62] Valizadeh B, Nguyen TN, Stylianou KC. Shape engineering of metal-organic frameworks. Polyhedron. 2018;**145**:1-15. DOI: 10.1016/j.poly.2018.01.004

[63] Ban J, Xu G, Zhang L, Lin H, Sun Z, Lv Y, et al. Mesoporous ZnO microcube derived from a metal-organic framework as photocatalyst for the degradation of organic dyes. Journal of Solid State Chemistry. 2017;**256**:151-157. DOI: 10.1016/j.jssc.2017.09.002

[64] Gao Q, Xu J, Bu X. Recent advances about metal-organic frameworks in the removal of pollutants from wastewater. Coordination Chemistry Reviews. In Press. DOI: 10.1016/j.ccr.2018.03.015

[65] He Y, Chen F, Li B, Qian G, Zhou W, Chen B. Porous metal-organic frameworks for fuel storage. Coordination Chemistry Reviews. 2018;**373**:167-198. DOI: 10.1016/j.ccr.2017.10.002

[66] Zhang J, Chen Z. Metal-organic frameworks as stationary phase for application in chromatographic separation. Journal of Chromatography A. 2017;**1530**:1-18. DOI: 10.1016/j.chroma.2017.10.065

[67] Qiu J, Zhang X, Feng Y, Zhang X, Wang H, Yao J. Modified metal-organic frameworks as photocatalysts. Applied Catalysis B: Environmental. 2018;**231**:317-342. DOI: 10.1016/j.apcatb.2018.03.039

[68] Ramezanalizadeh H, Manteghi F. Synthesis of a novel MOF/$CuWO_4$ heterostructure for efficient photocatalytic degradation and removal of water pollutants. Journal of Cleaner Production. 2018;**172**:2655-2666. DOI: 10.1016/j.jclepro.2017.11.145

[69] Wen J, Fang Y, Zeng G. Progress and prospect of adsorptive removal of heavy metal ions from aqueous solution using metal-organic frameworks: A review of studies from the last decade. Chemosphere. 2018;**201**:627-643. DOI: 10.1016/j.chemosphere.2018.03.047

[70] Hashemi B, Zohrabi P, Raza N, Kim K. Metal-organic frameworks as advanced sorbents for the extraction and determination of pollutants from environmental, biological, and food media. Trends in Analytical Chemistry. 2017;**97**:65-82. DOI: 10.1016/j.trac.2017.08.015

[71] Khan NA, Jhung SH. Adsorptive removal and separation of chemicals with metal-organic frameworks: Contribution of π-complexation. Journal of Hazardous Materials. 2017;**325**:198-213. DOI: 10.1016/j.jhazmat.2016.11.070

[72] Ahmed I, Jhung SH. Applications of metal-organic frameworks in adsorption/separation processes via hydrogen bonding interactions. Chemical Engineering Journal. 2017;**310**:197-215. DOI: 10.1016/j.cej.2016.10.115

[73] Fan Y, Zhang S, Qin S, Li X, Qi S. An enhanced adsorption of organic dyes onto NH_2 functionalization titanium-based metal-organic frameworks and the mechanism investigation. Microporous and Mesoporous Materials. 2018;**263**:120-127. DOI: 10.1016/j.micromeso.2017.12.016

[74] Sarker M, Song JY, Jhung SH. Adsorption of organic arsenic acids from water over functionalized metal-organic frameworks. Journal of Hazardous Materials. 2017;**335**:162-169. DOI: 10.1016/j. jhazmat.2017.04.044

[75] Zhang Q, Cui Y, Qian G. Goal-directed design of metal-organic frameworks for liquid phase adsorption and separation. Coordination Chemistry Reviews. In Press. DOI: 10.1016/j. ccr.2017.10.028

[76] Pi Y, Li X, Xia Q , Wu J, Li Y, Xiao J, et al. Adsorptive and photocatalytic removal of persistent organic pollutants (POPs) in water by metal-organic frameworks (MOFs). Chemical Engineering Journal. 2018;**337**:351-371. DOI: 10.1016/j.cej.2017.12.092

[77] Sharma VK, Feng M. Water depollution using metal-organic frameworks-catalyzed advanced oxidation processes: A review. Journal of Hazardous Materials. In Press. DOI: 10.1016/j.jhazmat.2017.09.043

[78] Wang S, Wang X. Multifunctional metal-organic frameworks for photocatalysis. Small. 2015;**11**:3097-3112. DOI: 10.1002/smll.201500084

[79] Seetharaj R, Vandana PV, Arya P, Ma S. Dependence of solvents, pH, molar ratio and temperature in tuning metal organic framework architecture. Arabian Journal of Chemistry. In Press. DOI: 10.1016/j.arabjc.2016.01.003

[80] Beg S, Rahman M, Jain A, Saini S, Midoux P, Pichon C, et al. Nanoporous metal organic frameworks as hybrid polymer-metal composites for drug delivery and biomedical applications.

Drug Discovery Today. 2017;**22**:625-637. DOI: 10.1016/j.drudis.2016.10.001

[81] Wang Y, Li L, Yan L, Cao L, Dai P, Gu X, et al. Continuous synthesis for zirconium metal-organic frameworks with high quality and productivity via microdroplet flow reaction. Chinese Chemical Letters. 2018;**29**:849-853. DOI: 10.1016/j. cclet.2017.09.057

[82] Panahi L, Naimi-Jamal MR, Mokhtari J, Morsali A. Mechanochemically synthesized nanoporous metal-organic framework $Cu_2(BDC)_2(DABCO)$: An efficient heterogeneous catalyst for preparation of carbamates. Microporous and Mesoporous Materials. 2017;**244**:208-217. DOI: 10.1016/j. micromeso.2016.10.031

[83] Majedi A, Davar F, Abbasi AR. Metal-organic framework materials as nano photocatalyst. International Journal of Nano Dimension. 2016;**7**:1-14. DOI: 10.7508/ijnd.2016.01.001

[84] Gangu KK, Maddila S, Mukkamala SB, Jonnalagadda SB. A review on contemporary metal-organic framework materials. Inorganica Chimica Acta. 2016;**446**:61-74. DOI: 10.1016/j. ica.2016.02.062

[85] Ren J, Dyosiba X, Musyoka NM, Langmi HW, Mathe M, Liao S. Review on the current practices and efforts towards pilot-scale production of metal-organic frameworks (MOFs). Coordination Chemistry Reviews. 2017;**352**:187-219. DOI: 10.1016/j. ccr.2017.09.005

[86] Pirzadeh K, Ghoreyshi AA, Rahimnejad M, Mohammadi M. Electrochemical synthesis, characterization and application of a microstructure $Cu_3(BTC)_2$ metal organic framework for CO_2 and CH_4 separation. Korean Journal of Chemical Engineering. 2018;**35**:974-983. DOI: 10.1007/s11814-017-0340-6

[87] Van Assche TRC, Denayer JFM. Fabrication and separation performance evaluation of a metal-organic framework based microseparator device. Chemical Engineering Science. 2013;**95**:65-72. DOI: 10.1016/j. ces.2013.03.006

[88] Yang H, Liu X, Song X, Yang T, Liang Z, Fan C. In situ electrochemical synthesis of MOF-5 and its application in improving photocatalytic activity of BiOBr. Transactions of Nonferrous Metals Society of China. 2015;**25**:3987-3994. DOI: 10.1016/ S1003-6326(15)64047-X

[89] Giménez-Marqués M, Hidalgo T, Serre C, Horcajada P. Nanostructured metal-organic frameworks and their bio-related applications. Coordination Chemistry Reviews. 2016;**307**:342-360. DOI: 10.1016/j.ccr.2015.08.008

[90] Wang C, Du X, Li J, Guo X, Wang P, Zhang J. Photocatalytic Cr(VI) reduction in metal-organic frameworks: A mini-review. Applied Catalysis B: Environmental. 2016;**193**:198-216. DOI: 10.1016/j.apcatb.2016.04.030

[91] Klimakow M, Klobes P, Rademann K, Emmerling F. Characterization of mechanochemically synthesized MOFs. Microporous and Mesoporous Materials. 2012;**154**:113-118. DOI: 10.1016/j. micromeso.2011.11.039

[92] Masoomi MY, Stylianou KC, Morsali A, Retailleau P, Maspoch D. Selective CO_2 capture in metal-organic frameworks with azine-functionalized pores generated by mechanosynthesis. Crystal Growth & Design. 2014;**14**:2092-2096. DOI: 10.1021/ cg500033b

[93] Chen Y, Xiao J, Lv D, Huang T, Xu F, Sun X, et al. Highly efficient mechanochemical synthesis of an indium based metalorganic framework with excellent water stability.

Chemical Engineering Science. 2017;**158**:539-544. DOI: 10.1016/j.ces.2016.11.009

[94] Seoane B, Castellanos S, Dikhtiarenko A, Kapteijn F, Gascon J. Multi-scale crystal engineering of metal organic frameworks. Coordination Chemistry Reviews. 2016;**307**:147-187. DOI: 10.1016/j.ccr.2015.06.008

[95] Zhu J, Li P, Guo W, Zhao Y, Zou R. Titanium-based metal-organic frameworks for photocatalytic applications. Coordination Chemistry Reviews. 2015;**359**:80-101. DOI: 10.1016/j.ccr.2017.12.013

[96] Abazari R, Mahjoub AR. Ultrasound-assisted synthesis of zinc(II)-based metal organic framework nanoparticles in the presence of modulator for adsorption enhancement of 2,4-dichlorophenol and amoxicillin. Ultrasonics Sonochemistry. 2018;**42**:577-584. DOI: 10.1016/j.ultsonch.2017.12.027

[97] Masoomi MY, Bagheri M, Morsali A. Porosity and dye adsorption enhancement by ultrasonic synthesized Cd(II) based metal-organic framework. Ultrasonics Sonochemistry. 2017;**37**:244-250. DOI: 10.1016/j.ultsonch.2017.01.018

[98] Abdollahi N, Masoomi MY, Morsali A, Junk PC, Wang J. Sonochemical synthesis and structural characterization of a new Zn(II) nanoplate metal-organic framework with removal efficiency of Sudan red and Congo red. Ultrasonics Sonochemistry. 2018;**45**:50-56. DOI: 10.1016/j.ultsonch.2018.03.001

[99] Batten MP, Rubio-Martinez M, Hadley T, Carey K, Lim K, Polyzos A, et al. Continuous flow production of metal-organic frameworks. Current Opinion in Chemical Engineering. 2015;**8**:55-59. DOI: 10.1016/j.coche.2015.02.001

[100] Stock N, Biswas S. Synthesis of metal-organic frameworks (mofs): Routes to various mof topologies, morphologies, and composites. Chemical Reviews. 2012;**112**:933-969. DOI: 10.1021/cr200304e

[101] He J, Li J, Du W, Han Q, Wang Z, Li M. A mesoporous metal-organic framework: Potential advances in selective dye adsorption. Journal of Alloys and Compounds. 2018;**750**:360-367. DOI: 10.1016/j.jallcom.2018.03.393

[102] Zhang J, Li F, Sun Q. Rapid and selective adsorption of cationic dyes by a unique metal-organic framework with decorated pore surface. Applied Surface Science. 2018;**440**:1219-1226. DOI: 10.1016/j.apsusc.2018.01.258

[103] Sanram S, Boonmak J, Youngme S. Ni(II)-metal-organic frameworks based on 1,4-phenylenedipropionic acid: Solvothermal syntheses, structures, and photocatalytic properties. Polyhedron. 2016;**119**:151-159. DOI: 10.1016/j.poly.2016.08.044

[104] Gao Y, Li S, Li Y, Yao L, Zhang H. Accelerated photocatalytic degradation of organic pollutant over metal-organic framework MIL-53(Fe) under visible LED light mediated by persulfate. Applied Catalysis B: Environmental. 2017;**202**:165-174. DOI: 10.1016/j.apcatb.2016.09.005

[105] Gao Y, Yu G, Liu K, Deng S, Wang B, Huang J, et al. Integrated adsorption and visible-light photodegradation of aqueous clofibric acid and carbamazepine by a Fe-based metal-organic framework. Chemical Engineering Journal. 2017;**330**:157-165. DOI: 10.1016/j.cej.2017.06.139

[106] Araya T, Chen C, Jia M, Johnson D, Li R, Huang Y. Selective degradation of organic dyes by a resin modified Fe-based metal-organic framework under visible light irradiation. Optical

Materials. 2017;**64**:512-523. DOI: 10.1016/j.optmat.2016.11.047

[107] Wang D, Jia F, Wang H, Chen F, Fang Y, Dong W, et al. Simultaneously efficient adsorption and photocatalytic degradation of tetracycline by Fe-based MOFs. Journal of Colloid and Interface Science. 2018;**519**:273-284. DOI: 10.1016/j.jcis.2018.02.067

[108] Abdpour S, Kowsari E, Moghaddam MRA. Synthesis of MIL-100(Fe)@MIL-53(Fe) as a novel hybrid photocatalyst and evaluation photocatalytic and photoelectrochemical performance under visible light irradiation. Journal of Solid State Chemistry. 2018;**262**:172-180. DOI: 10.1016/j.jssc.2018.03.018

[109] Lan Y, Lu Y, Ren Z. Mini review on photocatalysis of titanium dioxide nanoparticles and their solar applications. Nano Energy. 2013;**2**:1031-1045. DOI: 10.1016/j.nanoen.2013.04.002

[110] Patil RA, Devan RS, Liou Y, Ma Y. Efficient electrochromic smart windows of one-dimensional pure brookite TiO_2 nanoneedles. Solar Energy Materials & Solar Cells. 2016;**147**:240-245. DOI: 10.1016/j.solmat.2015.12.024

[111] Verbruggen SW. TiO_2 photocatalysis for the degradation of pollutants in gas phase: From morphological design to plasmonic enhancement. Journal of Photochemistry and Photobiology C: Photochemistry Reviews. 2015;**24**:64-82. DOI: 10.1016/j.jphotochemrev.2015.07.001

[112] Etacheri V, Valentin C, Schneider J, Bahnemann D, Pillai SC. Visible-light activation of TiO_2 photocatalysts: Advances in theory and experiments. Journal of Photochemistry and Photobiology C: Photochemistry Reviews. 2015;**25**:1-29. DOI: 10.1016/j.jphotochemrev.2015.08.003

[113] Singh S, Mahalingam H, Singh PK. Polymer-supported titanium dioxide photocatalysts for environmental remediation: A review. Applied Catalysis A: General. 2013;**462-463**:178-195. DOI: 10.1016/j.apcata.2013.04.039

[114] Singh R, Dutta S. A review on H_2 production through photocatalytic reactions using TiO_2/TiO_2-assisted catalysts. Fuel. 2018;**220**:607-620. DOI: 10.1016/j.fuel.2018.02.068

[115] Wang Y, He Y, Lai Q, Fan M. Review of the progress in preparing nano TiO_2: An important environmental engineering material. Journal of Environmental Sciences. 2014;**26**:2139-2177. DOI: 10.1016/j.jes.2014.09.023

[116] Khaki MRD, Shafeeyan MS, Raman AAA, Daud WMAW. Application of doped photocatalysts for organic pollutant degradation—A review. Journal of Environmental Management. 2017;**198**:78-94. DOI: 10.1016/j.jenvman.2017.04.099

[117] Cheng G, Xu F, Xiong J, Wei Y, Stadler FJ, Chen R. A novel protocol to design TiO_2-Fe_2O_3 hybrids with effective charge separation efficiency for improved photocatalysis. Advanced Powder Technology. 2017;**28**:665-670. DOI: 10.1016/j.apt.2016.12.004

[118] Cheng L, Qiu S, Chen J, Shao J, Cao S. A practical pathway for the preparation of Fe_2O_3 decorated TiO_2 photocatalyst with enhanced visible-light photoactivity. Materials Chemistry and Physics. 2017;**190**:53-61. DOI: 10.1016/j.matchemphys.2017.01.001

[119] Chang N, Zhang H, Shi M, Li J, Shao W, Wang H. Metal-organic framework templated synthesis of TiO_2@MIL-101 coreshell architectures for high-efficiency adsorption and photocatalysis. Materials Letters.

2017;**200**:55-58. DOI: 10.1016/j.matlet.2017.04.099

[120] Huang J, Song H, Chen C, Yang Y, Xu N, Ji X, et al. Journal of Environmental Chemical Engineering. 2017;**5**:2579-2585. DOI: 10.1016/j.jece.2017.05.012

[121] Dal'Toé ATO, Colpani GL, Padoin N, Fiori MA, Soares C. Lanthanum doped titania decorated with silver plasmonic nanoparticles with enhanced photocatalytic activity under UV-visible light. Applied Surface Science. 2018;**441**:1057-1071. DOI: 10.1016/j.apsusc.2018.01.291

[122] Colpani GL, Zanetti JT, Cecchin F, Dal'Toé A, Fiori MA, Moreira RFPM, et al. Carboxymethyl-β-cyclodextrin functionalization of TiO_2 doped with lanthanum: Characterization and enhancement of photocatalytic activity. Catalysis Science & Technology. 2018;**8**:2636-2647. DOI: 10.1039/C7CY02115A